# Plant Physiology®

# MAMP-elicited changes in amino acid transport activity contribute to restricting bacterial growth

Xiaomu Zhang (1), <sup>1</sup> Pramod Khadka (1), <sup>1</sup> Patryk Puchalski, <sup>1</sup> Joss D. Leehan (1), <sup>1</sup> Franco R. Rossi (1), <sup>1,2</sup> Sakiko Okumoto (1), <sup>3,†</sup> Guillaume Pilot (1) <sup>3</sup> and Cristian H. Danna (1) <sup>1\*,‡</sup>

- 1 Department of Biology, University of Virginia, Charlottesville, Virginia 22904, USA
- 2 Instituto Tecnológico Chascomús (INTECH), Universidad Nacional de General San Martín (UNSAM)—Consejo Nacional de Investigaciones Científicas y Técnicas (CONICET), Chascomús, Buenos Aires 7130, Argentina
- 3 School of Plant and Environmental Sciences, Virginia Tech, Blacksburg, Virginia 24061, USA

\*Senior author

Research Article

X.Z, P.K., P.P., J.D.L., and F.R.R. performed experiments. S.O. and G.P. provided Arabidopsis T-DNA insertional mutants. C.H.D. conceptualized the study and designed experiments. C.H.D. and X.Z. analyzed the data. C.H.D. wrote the manuscript. CHD, F.R.R. and G.P. edited the manuscript.

The author responsible for distribution of materials integral to the findings presented in this article in accordance with the policy described in the Instructions for Authors (https://academic.oup.com/plphys/pages/general-instructions) is Cristian H. Danna (cdanna@virginia.edu).

### **Abstract**

Plants live under the constant challenge of microbes that probe the environment in search of potential hosts. Plant cells perceive microbe-associated molecular patterns (MAMPs) from incoming microbes and activate defense responses that suppress attempted infections. Despite the substantial progress made in understanding MAMP-triggered signaling pathways, the downstream mechanisms that suppress bacterial growth and disease remain poorly understood. Here, we uncover how MAMP perception in Arabidopsis (*Arabidopsis thaliana*) elicits dynamic changes in extracellular concentrations of free L-amino acids (AA). Within the first 3 h of MAMP perception, a fast and transient inhibition of AA uptake produces a transient increase in extracellular AA concentrations. Within 4 and 12 h of MAMP perception, a sustained enhanced uptake activity decreases the extracellular concentrations of AA. Gene expression analysis showed that salicylic acid-mediated signaling contributes to inducing the expression of AA/H + symporters responsible for the MAMP-induced enhanced uptake. A screening of loss-of-function mutants identified the AA/H + symporter lysin/histidine transporter-1 as an important contributor to MAMP-induced enhanced uptake of AA. Infection assays in *Iht1-1* seedlings revealed that high concentrations of extracellular AA promote bacterial growth in the absence of induced defense elicitation but contribute to suppressing bacterial growth upon MAMP perception. Overall, the data presented in this study reveal a mechanistic connection between MAMP-induced plant defense and suppression of bacterial growth through the modulation of AA transport activity.

#### Introduction

Despite being sessile organisms that lack an adaptive immune system, plants are remarkably resistant to microbial infections. Leaf bacterial pathogens initiate infections upon breaching the stomatal barrier at the leaf surface and entering the water and nutrient-rich extracellular fluids that bathe the mesophyll cells, that is, the leaf apoplast (Xin and He, 2013). Early in the interaction, plant pattern-recognition receptors perceive a suite of microbial molecules or products of their activities, generally known as microbe-associated molecular patterns (MAMPs)

<sup>\*</sup>Author for correspondence: cdanna@virginia.edu

<sup>&</sup>lt;sup>†</sup>Present address: Department of Crop and Soil Science, Texas A & M, College Station, TX 77843, USA

and activate defense responses collectively known as MAMPtriggered immunity (MTI) (Gómez-Gómez et al., 1999; Nicaise et al., 2009). At the cellular level, early MTI responses include mitogen-activated protein-kinases activation, cytoplasmic Ca<sup>+2</sup> influx, extracellular alkalinization, production of reactive oxygen species, and genome-wide transcriptional reprogramming (Gómez-Gómez et al., 1999; Asai et al., 2002; Lecourieux et al., 2005). Late MTI responses include stomata closure, synthesis and accumulation of amino acid (AA)-derived secondary metabolites, and reinforcement of plant cell walls via callose and lignin deposition (Adams-Phillips et al., 2009; Clay et al., 2009; Chezem et al., 2017). Whereas MTI prevents most microbes from causing disease, pathogens have evolved mechanisms to counter MTI and produce infections. The bacterial pathogen Pseudomonas syringae pv. tomato (PstDC3000) suppresses MTI via the synthesis of the plant defense signaling antagonist molecule coronatine (COR) and the activity of type-3 secretion system (T3SS) effector proteins (T3E) (Hauck et al., 2003; Millet et al., 2010). PstDC3000 mutant strains that do not produce COR or deliver T3E fail to suppress MTI and only produce weak infections in otherwise susceptible host plants (Bender et al., 1987; Brooks et al., 2005; Zhang et al., 2008; Millet et al., 2010; Xin and He, 2013). In the leaf apoplast, invading bacteria spend the first few hours adjusting their metabolism to this rapidly changing environment (Yu et al., 2013; O'Leary et al., 2016). By modifying the leaf apoplast composition, plants might be able to suppress bacterial growth. In addition to polysaccharides, proteins, and complex secondary metabolites, the leaf apoplast of Arabidopsis (Arabidopsis thaliana) and tomato (Solanum lycopersicum) is rich in organic acids, polyamines, proteogenic AA, and gamma-aminobutyric acid (GABA) (Solomon and Oliver, 2001; Solomon and Oliver, 2002; Rico and Preston, 2008). Importantly, glucose, fructose, and several AA support PstDC3000 growth in vitro and have been shown to regulate the expression of T3SS genes in vivo in a concentration-dependent manner, suggesting an important function for these metabolites in controlling bacterial infections (Rahme et al., 1992; Rico and Preston, 2008; Park et al., 2010; Anderson et al., 2014; Chatnaparat et al., 2015a; Chatnaparat et al., 2015b; Yamada et al., 2016).

Among other metabolites, free AA and/or GABA accumulate in tomato leaf and leaf apoplast upon infection by Cladosporium fulvum or P. syringae (Solomon and Oliver, 2001) (Solomon and Oliver, 2002; O'Leary et al., 2016), suggesting a causal connection between accumulating metabolites and plant susceptibility to infections. It is unknown, however, if the accumulation of AA and GABA results from an ineffective plant defense response, or instead, from a microbial strategy to obtain nutrients and cause disease. These two equally plausible scenarios hinder the effort to define causality between metabolite content and pathogenicity. Previous studies showed that, among other plant metabolites that change their extracellular concentrations in response to MTI elicitation, organic acids, fructose, and glucose, can modulate bacterial virulence in a concentration dependent manner, thus providing a mechanistic explanation for MTI-mediated bacterial growth suppression. While MTI elicitation induces extensive changes in metabolite composition, only a few changing plant metabolites have been tested and reported to modulate bacterial growth *in planta*. Given the complexity of the MAMP-elicited metabolic changes, it would be expected that changes in concentrations of several metabolites could contribute to suppressing bacterial infections via multiple different mechanisms. Indeed, MTI suppresses the growth of both virulent and nonvirulent bacterial strains (e.g. that do not express an active T3SS), suggesting that suppressing virulence is not the only mechanism by which MTI suppresses bacterial growth (Tsuda et al., 2008; Nobori et al., 2018).

Salicylic acid (SA) is an intracellular signaling molecule that mediates transcriptional responses that elevate plant resistance to microbes. The signaling role of SA is well understood in defense processes initiated by cytosolic receptors, the so-called "resistance genes," that perceive T3E and initiate the SA-mediated onset of an enhanced pathogenresistant state known as effector-triggered immunity (ETI) (Delaney et al., 1994). The plant cells that initiate ETI often undergo programmed cell death (PCD), which manifests as a dried area of dead plant tissue at the site of attempted infection (Greenberg et al., 1994; Jirage et al., 1999; Coll et al., 2011). Importantly, Arabidopsis mutants that fail to accumulate SA in response to microbial invasion not only fail to induce cell death but are also highly susceptible to microbes that do not elicit ETI, indicating that the role of SA goes beyond controlling cell death and ETI (Lynne Reuber et al., 1998; Volko et al., 1998; Wildermuth et al., 2001). In Arabidopsis plants, SA levels increase 6 h after perceiving the MTI-eliciting synthetic peptide flg22, a 22 AA-long peptide containing the minimal epitope of the bacterial protein flagellin (Tsuda et al., 2008). Unlike wild-type plants, the SA biosynthesis mutant SA induction-deficient 2 (sid2) only partially activates the flg22-elicited transcriptional program and is less able to restrict P. syringae infections upon MTI elicitation (Wildermuth et al., 2001; Tsuda et al., 2009). Therefore, both MTI and ETI use SA-mediated signaling to induce resistance against microbes (Lu and Tsuda, 2021). However, it remains unclear which SA-signaling-controlled genes contribute to suppressing bacterial growth upon flg22-induced MTI.

Several lines of evidence suggest connections between AA transport activity and SA accumulation. Mutants or transgenic plants with enhanced AA export or compromised import activity accumulate high concentrations of SA (Liu et al., 2010; Yang et al., 2014a; Besnard et al., 2021). Lysin/histidine transporter-1 (*LHT1*) encodes an AA importer that localizes to the plasma membrane of leaf mesophyll cells where it plays an important role taking up Gln and other AA from the leaf apoplast (Hirner et al., 2006). When grown under long-day conditions, *Iht1-1* plants express high levels of the ammonium transporter-1;1 (*AMT1*;1), a gene induced in response to intracellular Gln deficiency (Gazzarrini et al., 1999; Liu et al., 2010). In such growth conditions, *Iht1-1* plants progressively accumulate SA and develop

spontaneous cell death lesions that are visible four weeks after germination, leading to a stunted rosette size and enhanced resistance to biotrophic pathogens (Hirner et al., 2006; Liu et al., 2010). The stunted phenotype of Iht1-1 plants was fully rescued when LHT1 was expressed under the control of a leaf mesophyll-cell-specific promoter, showing that loss of expression in the root is not responsible for the constitutive activation of defense responses (Hirner et al., 2006). Iht1-1 spontaneous cell death and pathogen phenotypes were rescued by the sid2 mutation, demonstrating that the buildup of SA is necessary to produce these phenotypes (Liu et al., 2010). Conversely, LHT1 mRNA accumulation increases upon SA treatment and pathogen inoculation (Liu et al., 2010). Similarly, several Arabidopsis genes encoding AA transporters are induced by pathogens and defense elicitors (Yang et al., 2014a), suggesting that AA transporters are potential effectors of MTI or the SA-mediated inducible defense.

The goal of the present study was to determine how MAMP perception impacts extracellular concentrations of AA and whether such changes contribute to plant immunity. Here, we report evidence that the perception of MAMPs leads to dynamic changes in AA transport activity and AA extracellular concentrations, identify transporters that contribute to changing extracellular concentrations of AA, define signaling pathways involved in their regulation, and describe the impact that AA concentration changes have on plant immunity and bacterial growth.

#### Results

### Elicitation of MTI induces dynamic changes in AA transport activity

Previous studies have shown that the onset of MTI is accompanied by changes in the composition of extracellular organic acids (Anderson et al., 2014). To understand if AA concentrations also change and how such changes contribute to plant immunity, we began by analyzing the AA content of exudates obtained from 10-day-old wild-type seedlings grown in liquid Murashige and Skoog (MS) medium and treated with flg22 for 24 h to elicit MTI. The concentration of total AA was assessed in samples of the MS medium containing seedling exudates at different time points after treatment. The concentration of total AA in the exudates rose within the first 4 h, then declined and remained low between 12 h and 24 h after MAMP perception (Figure 1A). Targeted mass spectrometry analysis of exudates showed that, the concentration of most extracellular AA changed in response to flg22 perception, except Asp and Glu. While the concentration of most AA increased significantly 4 h post-flg22 treatment, Arg, Gly, Lys, Thr, and Tyr show a similar upward trend but did not increase significantly. Twenty-four hours post-treatment, the concentration of all extracellular AA detected (except for Asp and Glu) decreased significantly in exudates of flg22-treated compared to mock-treated seedlings (Table 1). We hypothesized that changes in AA concentrations in exudates would be

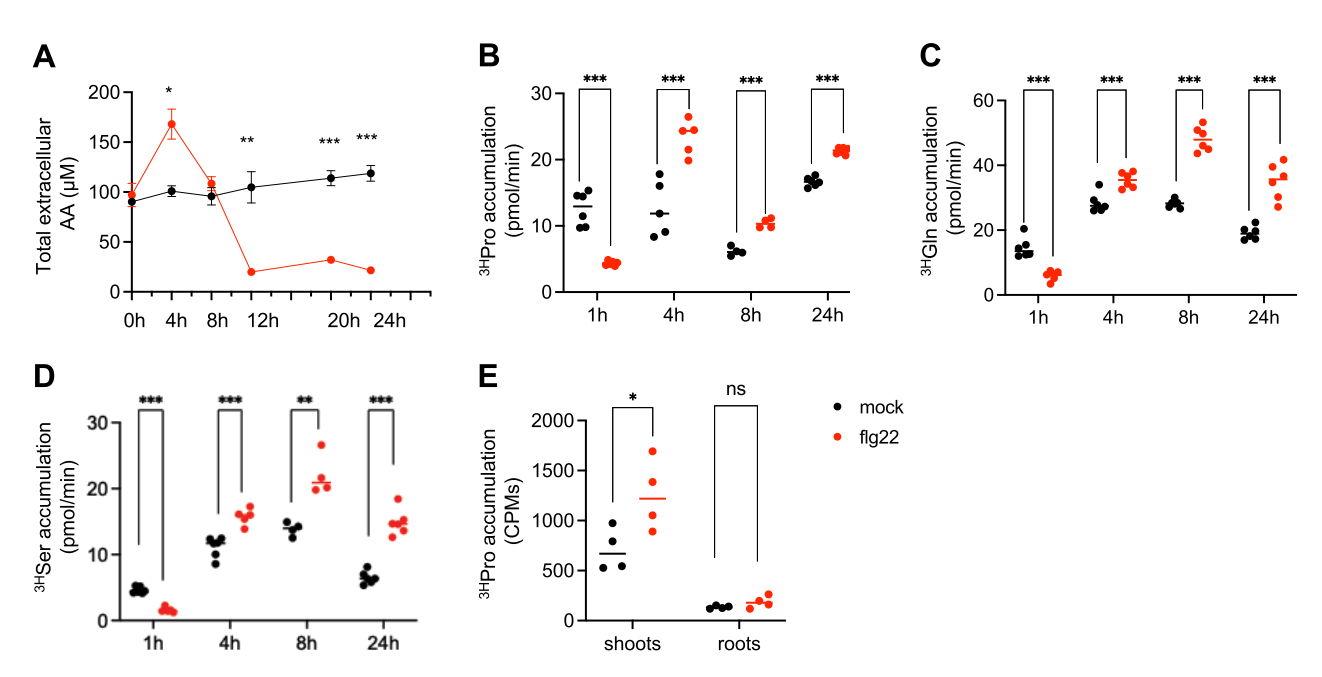


**Figure 1** MAMP perception induces changes in AA transport activity that modulate extracellular AA concentrations. A, Mean  $\pm$  standard error of the mean (sem) (n = 3) of total AA concentrations in the liquid exudates of mock- (black) or flg22-treated (red) wild-type seedlings. B, <sup>3H</sup>Pro, (C) <sup>3H</sup>Gln, and (D) <sup>3H</sup>Ser uptake rates of wild-type seedlings pre-treated with water (black) or flg22 (red) for 1 h, 4 h, 8 h, or 24 h prior to assessing the uptake activity. n = 6 replicates of 10 seedlings per point. E, Accumulation of <sup>3H</sup>Pro (CPM = count per minute) in roots and shoots of seedlings pretreated with water (black) or flg22 (red) for 24 h. Intact seedlings were allowed to take up <sup>3H</sup>Pro for 3 h, washed and severed below the hypocotyl, and CPMs were quantified separately in shoots and roots. n = 4 replicates of 10 seedlings per point. (ns) nonsignificant. Data analysis: t-test (A); Welch t test (B, C, D, and E). \*, \*\*, and \*\*\* indicate statistically significant differences at P-values of < 0.05, < 0.01, and < 0.001, respectively.

Table 1 Concentration of AA in exudates of wild-type seedlings (mean ± standard error of mean) assessed by mass spectrometry

		4 h post-	nt				24 h post-				
	Mock (n = 6)		flg22 $(n = 6)$				Mock (n = 8)		flg22 (n = 8)		
Amino Acids	Mean (μM)	Standard error of the mean	Mean (μM)	Standard error of the mean	Adjusted P-value M versus F		Mean (μM)	Standard error of the mean	Mean (μM)	Standard error of the mean	Adjusted <i>P-</i> value M versus F
Ala*	5.42	0.10	12.57	0.25	1.24E-03	Ala*	3.24	0.56	0.63	0.09	2.19E-03
Arg	0.04	0.00	0.37	0.03	6.70E-02	Arg*	0.21	0.02	0.11	0.02	3.39E-03
Asn*	0.10	0.00	0.40	0.02	2.49E-02	Asn*	36.79	3.96	8.02	1.72	6.90E-05
Asp	5.43	0.22	4.03	0.13	3.05E-01	Asp	2.79	0.66	1.77	0.47	2.32E-01
Cys	ND	ND	ND	ND		Cys	0.05	0.02	ND	ND	
Glu	10.03	0.29	11.86	0.28	3.82E-01	Glu	6.06	0.78	8.24	1.97	3.30E-01
Gln*	71.42	0.89	123.97	0.70	5.00E-06	Gln*	62.28	11.84	16.66	3.66	5.79E-03
Gly	1.84	0.07	4.13	0.20	7.77E-02	Gly*	4.35	1.00	1.19	0.21	1.61E-02
His*	0.58	0.01	1.05	0.01	2.00E-06	His*	3.00	0.49	0.30	0.15	6.29E-04
lle*	3.72	0.03	7.81	0.14	1.77E-03	lle*	1.13	0.25	0.19	0.04	6.16E-03
Leu*	2.44	0.02	6.65	0.13	1.30E-03	Leu*	1.93	0.51	0.10	0.03	8.75E-03
Lys	0.02	0.00	0.10	0.01	7.68E-02	Lys*	0.44	0.05	0.12	0.02	2.21E-04
Met*	0.07	0.00	0.30	0.01	1.17E-02	Met	0.06	0.02	0.02	0.00	9.51E-02
Phe*	0.92	0.01	3.72	0.06	2.54E-04	Phe*	0.54	0.12	0.17	0.03	1.84E-02
Pro*	0.79	0.01	2.32	0.04	3.43E-04	Pro*	2.36	0.41	0.00	0.06	5.47E-04
Ser*	6.15	0.16	12.54	0.39	2.09E-02	Ser*	7.48	0.90	1.80	0.36	2.28E-04
Thr	3.05	0.06	4.31	0.12	9.32E-02	Thr*	2.36	0.39	0.88	0.24	6.95E-03
Try*	0.42	0.00	0.80	0.01	1.51E-04	Try*	0.23	0.06	0.04	0.01	1.24E-02
Tyr	0.58	0.01	1.23	0.05	5.30E-02	Tyr*	0.34	0.07	0.08	0.02	5.34E-03
Val*	11.97	0.09	20.52	0.17	3.10E-05	Val*	5.47	1.42	0.36	0.14	8.67E-03

Asterisks indicate AA whose concentrations increased or decreased significantly (P < 0.05 in bold font) at 4 h (n = 6) and 24 h (n = 8) after flg22 treatment, respectively. (ND) not detected. More than five independent experiments produced similar results. Data were analyzed with Welch t-test; P-values were adjusted by the two-stage step-up false discovery rate method (Q = 0.01).

dependent on changes in AA transport activity across the plasma membrane. To test this hypothesis, we assessed AA transport activity in wild-type seedlings using radiolabeled Pro, Gln, and Ser, three AA whose concentrations increased at 4 h and decreased significantly 24 h after MTI elicitation. The AA uptake activity of mock- and flg22-treated seedlings was assessed at several time points between 1 h and 24 h after treatment by removing the liquid medium, washing the seedlings, and incubating the seedlings in a mix of 100-µM cold Pro, Gln, or Ser, and 3.7 kBq of the corresponding radiolabeled AA. Wild-type seedlings were allowed to take up <sup>3H</sup>Pro for 3 h, and Gln or Ser for 30 min. The perception of flg22 inhibited 3HPro, 3HGIn, and 3HSer uptake as soon as 1 h post-elicitation but induced their uptake at later time points, mirroring the concentrations of extracellular AA detected in seedling exudates along the same 24 h period (Figure 1, B-D). These data suggest that changes in AA transport activity contribute to changing extracellular concentrations of AA in response to flg22 perception. To test the implication of MAMP perception in this response, AA exudation and transport were measured in the fls2-1 (SALK 026801) and efr-1 (SALK 044334) mutants, respectively lacking the receptor for flg22 and elf26, a 26 AA-long synthetic peptide containing the minimal epitope of the bacterial ribosome elongation factor-TU. Like flg22, treatments with elf26 for 24 h induced an enhanced AA uptake activity in wild-type seedlings (Supplemental Figure S1). Unlike wild-type seedlings, fls2-1 and efr-1 did not show enhanced uptake of AA 24 h after flg22 or -elf26 treatments, respectively (Supplemental Figure S1). These data indicate that changes in AA transport are dependent on signaling processes initiated by MAMP receptors and suggest that changes in AA transport activity are a conserved response to MAMP perception. To determine which organ/s contributed to flg22-induced enhanced AA uptake, seedlings were grown in liquid MS medium, treated with water or flg22 for 24 h, allowed to take up Pro for 3 h, and sectioned below the hypocotyl to assess <sup>3H</sup>Pro accumulation in shoots and roots separately. This approach revealed that shoots contributed with most of the basal and the flg22-induced enhanced uptake (Figure 1E). In a similar experiment, seedlings were treated with water or flg22 for 8 h, sectioned below the hypocotyl, and roots and shoots were then allowed to take up <sup>3H</sup>Pro separately. Here again, while shoots uptake was increased by flg22 pretreatment, roots showed less uptake activity overall and did not show enhanced Pro uptake in response to flg22 treatment (Supplemental Figure S2). These data indicate that MAMP-elicited changes in AA transport in green tissues, and not root tissues, are responsible for the modulation of the concentrations of extracellular AA detected in seedling exudates.

### MAMP-perception elicits an enhanced uptake of AA via the activation of AA/H \* symporters

In most physiological conditions, cytosolic concentrations of AA are higher than those found outside the cells. Cells maintain a high cytosolic concentration of AA via both the de novo biosynthesis and the reuptake of AA that leak out of the cells (Okumoto and Pilot, 2011; Yang et al., 2020; Yao et al., 2020). Cells take up AA against a concentration

gradient via plasma membrane-localized AA/H+-coupled symporters (AA/H<sup>+</sup> symporters) whose activity depend on the H<sup>+</sup> electrochemical gradient generated by the plasma membrane H+-ATPases (Bush and Langston-Unkefer, 1988). To test whether the MAMP-elicited enhanced uptake of AA requires H<sup>+</sup> gradient, and hence AA/H<sup>+</sup> symporters, <sup>3H</sup>Pro accumulation was assessed in seedlings pretreated for 24 h with water or flg22 and then treated with carbonyl cyanide m-chlorophenyl hydrazine (CCCP) for 40 min before the start of the AA uptake assay. CCCP, a protonophore that dissipates the H<sup>+</sup> gradient across all membranes, quickly inhibits adenosine triphosphate (ATP) synthesis and the H<sup>+</sup>coupled transport of AA (Bush and Langston-Unkefer, 1988; Hirner et al., 2006). CCCP inhibited both the basal and the MTI-elicited uptake of Pro (Figure 2A), highlighting the role of AA/H + symporters in the MTI-elicited enhanced AA uptake activity 24 h post-treatment. Expectedly, the inhibition of AA uptake with CCCP produced a significant increase in extracellular AA concentrations (Figure 2B), showing that seedlings continued exporting AA out of the cells through passive transporters when the active uptake of AA was inhibited. To identify transporters that would contribute to AA uptake during MTI progression, we mined published Arabidopsis gene expression data for flg22-induced AA/H<sup>+</sup> symporters and found eleven genes induced in seedlings at either 1 h or 3 h after flg22 perception (Denoux et al., 2008). Seven of these AA/H+ symporters were at least 1.5-fold induced (P < 0.05) by flg22 treatment in Arabidopsis leaves: two members of the AA permease (AAP) subfamily, three members of the LHT subfamily, one member of the proline transporter (ProT) subfamily, and one member of the cationic AA transporter (CAT) subfamily (Supplemental Table S1). Ten-day-old seedlings grown in liquid medium were treated with water (mock treatment) or flg22 and RNA samples were collected at different time points. nanoString hybridization and reverse transcription-quantitative polymerase chain reaction (RT-qPCR) confirmed that wildtype seedlings induced the expression of these AA transporters 8 h after exposure to flg22 (Figure 2C), a time point when the uptake of Pro, Gln, and Ser was higher than in mock-treated seedlings (see Figure 1, C, D, and E). To assess the contribution of these genes to changes in AA transport during MTI progression, we tested the basal and the flg22induced uptake of AA in their corresponding loss-offunction mutants. 3HPro was used as a tracer for uptake in aap3-1 (SALK\_148822), Iht1-1 (SALK\_034566), and prot2-1 (SALK\_067508) since the corresponding transporters were previously confirmed to transport Pro (Rentsch et al., 1996; Okumoto et al., 2002; Hirner et al., 2006). AA uptake in cat1-1 (SALK\_087921) was assessed with <sup>3H</sup>Gln, because CAT1 was shown to transport Gln but not Pro (Su et al., 2004). Due to the lack of information on LHT7 and LHT10 substrate specificity, we tested <sup>3H</sup>Pro and <sup>3H</sup>Gln transport in Iht7-1 (SALK\_027033), Iht7-2 (SALK\_043012), and Iht10-1 (SALK 114616). Of the eight mutants tested, only Iht1-1 uptake activity was lower than in the wild-type and did not

increased 24 h after flg22 treatment (Figure 2, D and E). In addition, Iht1-1 was the only mutant for which the AA content in seedling exudates was not decreased by flg22 treatment, in agreement with its inability to enhance AA uptake in the same conditions (Figure 3B and Supplemental Figure S3). The Iht1-1 mutant also lacked the flg22-elicited enhanced uptake of <sup>3H</sup>Ser (Supplemental Figure S4A) and the elf26-elicited increase in <sup>3H</sup>Pro, <sup>3H</sup>Gln, and <sup>3H</sup>Ser uptake (Supplemental Figure S4, C, D, and E). As previously shown by Hirner et al. (2006), the uptake of glucose, which also depends on an intact H<sup>+</sup> gradient across the plasma membrane, was similar in wild-type and Iht1-1 in mock conditions (Supplemental Figure S4B), confirming that the observed AA transport defects are not caused by an altered H<sup>+</sup> electrochemical gradient or another general transport defect in Iht1-1. To rule out MAMP perception or signaling defects in *lht1-1*, we assessed the transcriptional response to flg22 perception. RT-qPCR data showed that Iht1-1 and wildtype seedlings induced the expression of canonical flg22responsive genes to a similar extent 3 h after flg22 treatment (Figure 2F). Similarly, AA/H+ symporters were induced to a similar extent in Iht1-1 and wild-type seedlings 3 h after flg22 treatment (Figure 2F). These data show that flg22 perception and signaling are intact the Iht1-1 mutant. Overall, the data presented in this section demonstrate that the flg22-induced AA/H<sup>+</sup> symporter LHT1 is necessary to drive the enhanced uptake of AA elicited by flg22 and elf26.

### Salicylic acid-mediated signaling contributes to AA uptake regulation

While the impact of AA transport defects on SA accumulation has been reported in several studies, the impact of SA signaling on AA transport activity has been less documented. In beet (Beta vulgaris) leaves, SA treatment inhibited the uptake of AA in a dose-dependent manner (Bourbouloux et al., 1998). This precedent, together with previously published connections between SA accumulation and the compromised AA transport in Iht1-1 (Liu et al., 2010), prompted us to test if SA accumulation contributes to inhibiting AA uptake of *lht1*. To this end, we assessed the uptake of AA in the Iht1-1, sid2-2 double mutant (I1s2), which no longer accumulates an excess of SA compared to Iht1-1 (Liu et al., 2010). Both, Iht1-1 and I1s2 showed a similarly lower uptake of <sup>3H</sup>Pro in mock conditions compared to the wild-type, and flg22 treatment had no effect on Pro uptake in either genotype, showing that SA does not contribute to the impaired AA uptake in Iht1-1 (Figure 3A). Interestingly, Pro uptake did not increase in response to flg22 treatment in the sid2-2 mutant (Figure 3A), suggesting that the SA signaling plays a role in the flg22-induced enhanced uptake of AA. Consistently with their compromised uptake, the concentration of extracellular AA in Iht1-1 and 11s2 did not decrease in response to flg22 perception (Figure 3B). In addition, sid2-2 showed a lower concentration of extracellular AA in exudates of mock-treated compared to wild-type seedlings (Figure 3B). Measurement of Gln

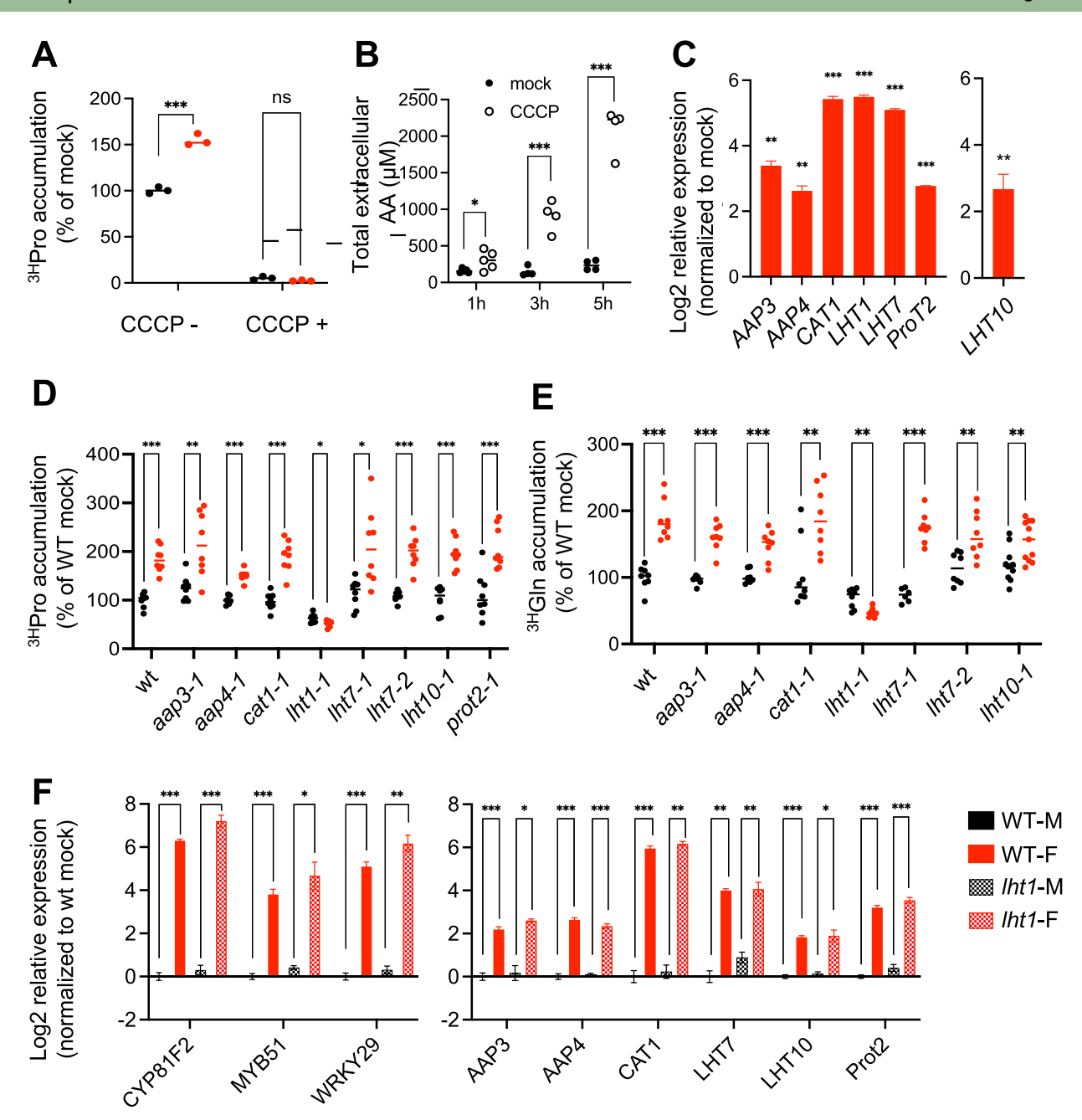


**Figure 2** LHT1 drives the uptake of AA in both mock and MTI-elicited seedlings. A, Wild-type (wt) seedlings were treated for 24 h with water (black) or flg22 (red).  $^{3H}$ Pro uptake was assessed with or without 100-μM CCCP to inhibit active transport. n=3 replicates of 10 seedlings per point. Two independent experiments produced identical results. B, Concentration of total AA in exudates of wild-type (wt) seedlings treated with water or 100-μM CCCP. Total AA were quantified in exudates 1 h, 3 h, and 5 h post-treatment. n=4 replicates of 10 seedlings per point. Two independent experiments produced identical results. C, Mean  $\pm$  sem (n=3) relative expression of AA/H $^+$  symporters in wt seedlings 8 h after flg22 treatment; messenger RNA (mRNA) levels were assessed with nanoString hybridizations and analyzed with the nSolver software. LHT10 expression was quantified via RT-qPCR. Total RNA samples were obtained from 15 10-day-old seedlings 8 h after flg22 treatment from three independent experiments. D,  $^{H3}$ Pro and (E)  $^{3H}$ Gln uptake activity in wt and insertional mutants of candidate genes after mock- (black) or flg22 treatment (red). Replicates of 10 seedlings per sample (n=8). F, Mean  $\pm$  sem relative expression of early canonical flg22-induced genes (left) and AA/H $^+$  symporters (right). Total RNA samples were obtained from 15 10-day-old seedlings 3 h post-treatment from three independent experiments (n=3). Data analysis: Welch t test (A); t test (B and F); one-sample t test (C); multiple Welch t test (D and E). \*, \*\*, and \*\*\* indicate statistically significant differences at t-values of t-valu

uptake 24 h after flg22 treatment corresponded well with these data: no increase in Gln uptake was observed for *lht1-1* and *l1s2*, while *sid2-2* showed less Gln uptake activity than the

wild-type in both mock and flg22 conditions (Supplemental Figure S5). This result suggests that SA exerts a positive action on the regulation of AA uptake in both non-elicited and

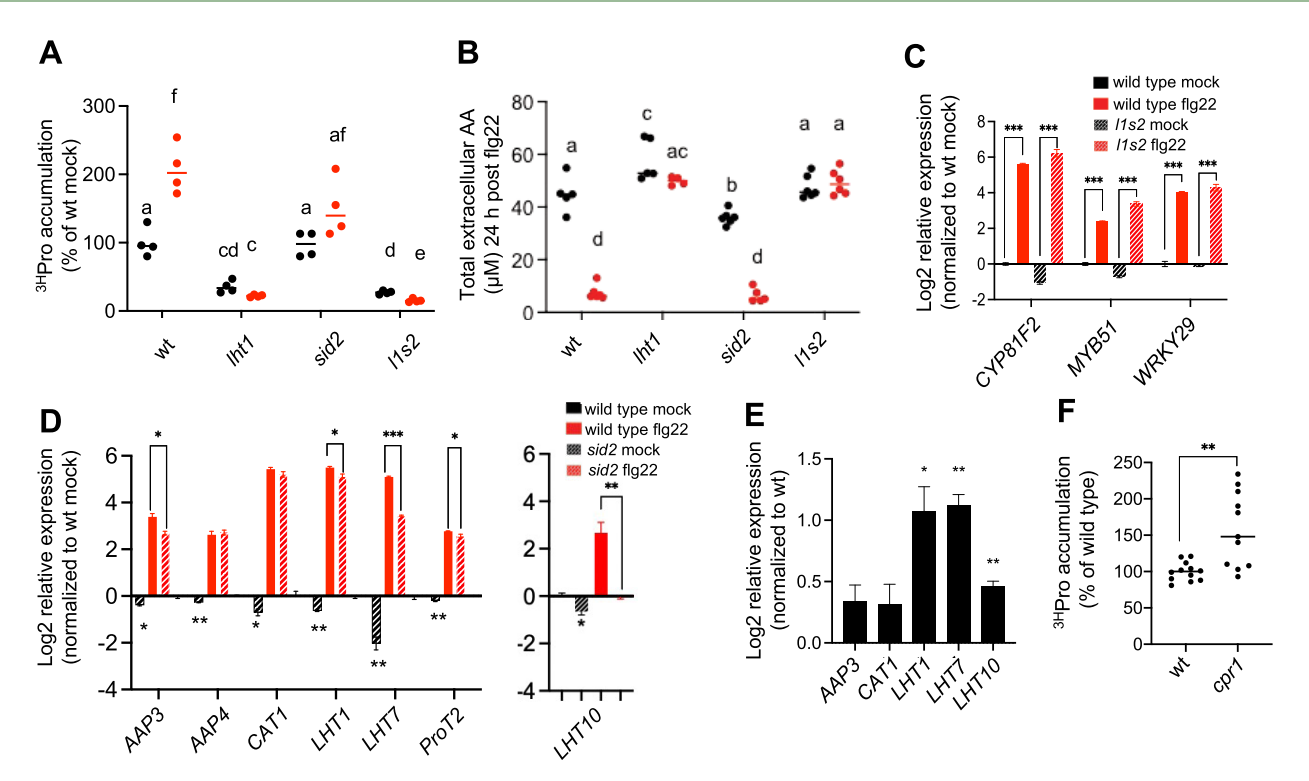


**Figure 3** Salicylic acid positively modulates the late MAMP-induced enhanced AA uptake. A,  $^{3H}$ Pro uptake 24 h after mock (black) or flg22 (red) treatment. Replicates of 10 seedlings per point (n=4). Four independent experiments yielded similar results. B, Concentration of total extracellular AA in exudates of seedlings 24 h after mock (black) or flg22 (red) treatment. Replicates of 10 seedlings per sample (n = 5 for wt, lth1-1, and sid2-2; n = 6 for lht1-sid2 double mutant). C, Mean  $\pm$  sem relative expression of early canonical flg22-induced genes in wt (solid) or l1s2 (stripped) seedlings 3 h after mock (black) or flg22 (red) treatment. Total RNA samples were obtained from 15 10-day-old seedlings 3 h post-treatment from three biological replicates (n = 3) and gene expression was assessed via RT-qPCR. D, Mean  $\pm$  sem relative expression of AA/H $^+$  symporters in wt (solid) or sid2 (stripped) seedlings 8 h after mock (black) or flg22 (red) treatment. Total RNA samples were obtained from 15 10-day-old seedlings 8 h post-treatment from three biological replicates (n = 3). Gene expression was assessed via nanoString hybridization except for LHT10 which was quantified by RT-qPCR. E, Mean  $\pm$  sem relative expression of flg22-induced, SA-regulated AA/H $^+$  symporters in cpr1 seedlings normalized to the wt levels. Total RNA samples were obtained from 15 10-day-old seedlings 8 h post-treatment from three biological replicates (n = 3) and gene expression was assessed by RT-qPCR. Two independent experiments yielded similar results. F, n Pro uptake in nontreated n seedlings. Replicates of 10 seedlings per sample (n = 12). Data analysis: Welch and Brown-Forsythe ANOVA tests (A); two-way ANOVA test (B); multiple n tests (C); n test (D) except for LHT10 Welch n test; one-sample n test (E); Welch n test (F). \*, \*\*, \*\*, and \*\*\* indicate statistically significant differences at n P-values of n = 0.001, and n = 0.001, respectively. Different letters in (A) and (B) indicate stat

MTI-elicited conditions. The response to flg22, assessed as the expression of the flg22-induced markers *CYP81F2*, *MYB51*, and *WRKY29*, was similar in the wild-type and *l1s2* seedlings 3 h post-treatment (Figure 3C), showing that neither the *lht1-1* nor the *sid2-2* mutations affected early flg22 signaling.

To test for a potential role for SA in the transcriptional regulation of AA transporters following flg22 treatment, the expression of the seven flg22-induced AA/H<sup>+</sup> symporters was assessed in the *sid2-2* mutant 8 h after flg22-treatment. The expression of AAP3, LHT1, LHT7, ProT2, and LHT10 was lower in *sid2-2* compared to wild-type in non-elicited conditions, and AAP3, LHT7, ProT2, and LHT10 were not induced in *sid2-2* to the same extent as in wild-type seedlings in response flg22 perception. These data suggest that, in addition to LHT1, AAP3, LHT7, ProT2, and LHT10, play a role, albeit minor, in mediating the AA uptake activity controlled by SA in both non-elicited and MTI-elicited conditions (Figure 3D). Based on this evidence, we hypothesized that mutants that constitutively accumulate

high levels of SA would display a constitutively high expression of AA/H<sup>+</sup> symporters and enhanced AA uptake activity compared to wild-type plants. Indeed, the "Constitutive Expressor of PR genes-1" (*cpr1*) mutant that overaccumulates SA (Bowling et al., 1994), expresses higher levels of *LHT1*, *LHT7*, and *LHT10* mRNAs compared to wild-type seedlings (Figure 3E). In addition, <sup>3H</sup>Pro uptake in *crp1* was significantly higher than in wild-type seedlings (Figure 3F), confirming our hypothesis. These data show that SA-mediated signaling positively regulates the uptake of AA both in control and flg22-elicited conditions. In addition, the AA transport activities corresponded tightly with the concentration of extracellular AA in exudate in all the conditions tested.

### MAMP perception transiently inhibits AA uptake independently of SA signaling

Having established that LHT1 and flg22-elicited SA-mediated responses are important in activating AA uptake and

lowering extracellular AA concentrations 24 h after flg22 treatment, we assessed the role of SA and AA/H<sup>+</sup> symporters in the inhibition of AA uptake observed 1 h after flg22 perception, when the concentration of extracellular AA increases in the exudates (Figure 1A). While the decrease in Pro uptake in the wild-type seedlings 1 h after elicitation was absent in fls2, the inhibition was still present in sid2-2, suggesting that this response depends on the receptormediated perception of flg22, but not on SA-mediated signaling (Figure 4A). Previously published gene expression data (Denoux et al., 2008) and our results showed that the expression of all the AA transporters tested was induced 1 h, 3 h, and 8 h after flg22 treatment (Supplemental Table S1 and Supplemental Figure S6A and B; Figure 2C). Therefore, the inhibition of AA uptake 1 h after flg22 perception does not correspond with the expression of AA/H<sup>+</sup> symporters. suggesting that other regulatory mechanisms might be involved. Leaf mesophyll cells are in direct contact with bacterial pathogens that colonize the leaf apoplast. Hence, to provide a more direct estimation of the changes that take place in the leaf apoplast in response to flg22, we measured AA transport properties of mesophyll protoplasts. Like seedlings (Figure 1A; Supplemental Figure S1), the perception of flg22 by wild-type protoplasts induced the expression of MTI response markers (Supplemental Figure S7A) and elicited an FLS2-dependent inhibition of AA uptake at 1 and 3 h post-treatment (Figure 4B; Supplemental Figure S7B). As shown previously, while Iht1-1 protoplasts were compromised for Pro uptake (Hirner et al., 2006), they still responded to flg22 treatment by decreasing the uptake even further (Figure 4C). These data suggest that, in addition to LHT1, other transporters must be responsible for the background uptake activity in Iht1-1 protoplasts. The role of SAmediated signaling in AA uptake was assessed in leaf protoplasts of sid2-2 and of the "Non-expressor of Pathogenesis-Related genes-1" (npr1) mutant, a signaling mutant that accumulates wild-type levels of SA, but fails to induce SAmediated transcriptional responses (Cao et al., 1997). In nonelicited conditions, <sup>3H</sup>Pro uptake was lower in sid2-2 and npr1 protoplasts compared to the wild-type (Figure 4D). The perception of flg22 still inhibited Pro uptake in both mutants to a similar extent as in wild-type protoplasts. These data show that SA-signaling is necessary for basal AA uptake activity in mesophyll cells in mock conditions, and confirmed that, like in seedlings, the perception of flg22 inhibits the uptake of AA at earlier time points via an SA-independent mechanism.

### MAMP-induced changes in AA transport contribute to restricting bacterial growth

Both seedlings and adult plants perceive flg22 and mount defense responses that suppress P. syringae infection (Zipfel et al., 2004; Danna et al., 2011). To test the effects of flg22induced changes in AA transport activity and extracellular concentrations of AA on the bacterial growth, P. syringae pv. maculicola ES4326 (PsmES4326) growth was measured in seedling exudates obtained from mock or flg22-treated wildtype seedlings. Pathogen growth was slower in exudates of flg22-treated seedlings (Figure 5A). This result was reminiscent of those obtained when the pathogen infected seedlings in liquid medium (Danna et al., 2011), suggesting that the conditions that determine bacterial growth are, to some extent, similar in seedlings and exudates. To assess the contribution of the lower AA content in exudates of flg22treated seedlings on bacterial growth, seedling exudates obtained 24 h after mock or flg22 treatment were supplemented with individual AA, and PsmES4326 growth rates were determined as doubling time. In the conditions tested, Asn, Glu, Gln, Leu, and Pro were able to rescue bacterial growth (Supplemental Table S2), suggesting that decreased concentrations of Asn, Gln, Leu, and Pro in the exudates of flg22-elicited seedlings (Table 1) contribute to limiting PsmES4326 growth. We thus reasoned that grinding flg22treated wild-type seedlings would make the sequestered AA available to support bacteria growth, thus allowing bacteria to grow similarly in both mock-elicited and flg22-elicited seedling lysates. Ten-day-old seedlings grown in liquid MS medium were treated with water (mock) or flg22 for 24 h and then removed from the MS medium and ground. In the lysates of flg22-treated seedling, PsmES4326 replicated

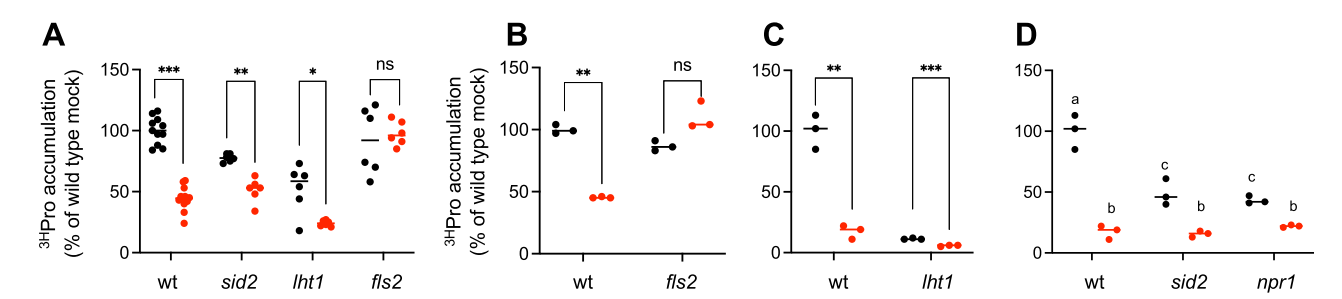


**Figure 4** MAMP perception rapidly and transiently inhibits the uptake of AA in a salicylic acid-independent manner. A,  $^{3H}$ Pro uptake in wt and mutant seedlings 1 h after mock (black) or flg22 (red) treatment. Replicates of 10 seedlings per sample (n = 12 for wt; n = 6 for mutants). B–D,  $^{3H}$ Pro accumulation in mesophyll protoplasts of wt plants and the fls2 (B), lht1-1 (C), sid2-2, and npr1 (D) mutants. Protoplasts were treated for 3 h with flg22 (red) or water (black) before Pro uptake assessment. Replicates of  $1 \times 10^{+6}$  protoplast cells per sample (n = 3). Data analysis: Welch t test (A, B, and C); t test (D). \*, \*\*, and \*\*\* indicate statistically significant differences at t-values of t-values of

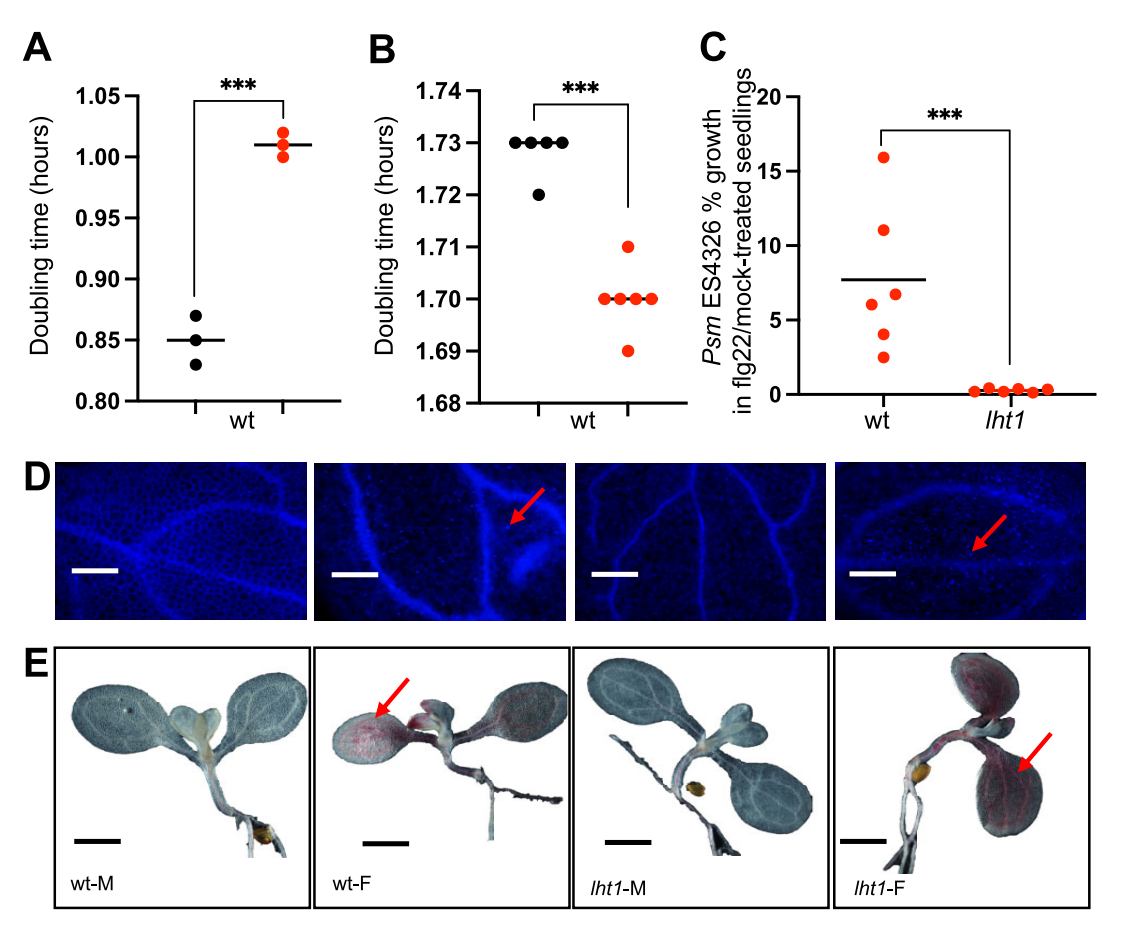


Figure 5 The rapid and transient MAMP-elicited AA uptake inhibition contributes to suppressing bacterial growth. A, Bacterial doubling time in exudates was obtained 24 h after mock (black) or flg22 (red) treatment of wt seedling. Replicates of bacterial growth in exudates were obtained from 15 10-day-old seedlings from three biological replicates (n = 3). B, Bacterial doubling time in lysates obtained from wt seedlings 24 h after mock (black) or flg22 (red) treatment. Replicates of bacterial growth in seedling lysates were obtained from 15 10-day-old seedlings from three biological replicates (n = 3). C, Percentage of bacterial growth in flg22-treated wt or lht1-1 (lht1) seedlings normalized by growth in mock-treated seedlings 30 h after inoculation. Replicates of bacterial growth in 15 10-day-old seedlings from three biological replicates (n = 3). D, Callose and (E) lignin deposition in wt and lht1-1 (lht1) mock- (M) or flg22- (F) treated seedlings grown for 6 days in liquid MS and stained 2 days after treatment. Bar size = 0.05 mm. Arrows indicate callose or lignin deposits. Images were taken with a Zeiss Axio Imager microscope and a color CCD camera. Bar size = 1mm. Data analysis: t test (A and B); Welch t test (C). \*, \*\*, and \*\*\* indicate statistically significant differences at t-values of t-value

faster than in mock-elicited seedling lysates, suggesting that MTI-elicited seedlings actively suppress bacterial growth by modifying the apoplast composition, perhaps via sequestering AA inside the cell (Figure 5B).

To directly test if and how flg22-elicited changes in AA concentration contribute to plant defense and bacterial growth, wild-type and *lht1-1* seedlings were grown in liquid MS medium for 10 days and treated with water or flg22 for 24 h before inoculation with *Psm*ES4326. The infection proceeded in conditions identical to those used for plant growth. Thirty hours later, seedlings were removed from liquid MS and ground to assess infection. In good agreement with the hypothesis stated above, *lht1-1* seedlings allowed for enhanced bacterial growth in mock-treated seedlings (Supplemental Figure S8), possibly due to the higher concentration of extracellular AA available to support growth in *lht1-1*. Upon flg22 perception, however, bacterial growth was suppressed to a higher extent in *lht1-1* than in wild-type

seedlings (Figure 5C; Supplemental Figure S8). As Iht1-1 does not lower the concentration of extracellular AA in response to flg22 perception, this result falsifies the hypothesis that PsmES4326s growth positively corresponds with the abundance of extracellular AA upon the elicitation of MTI. Adult Iht1-1 plants are smaller than wild-type and constitutively express SA-mediated enhanced resistance to P. syringae, which could explain the exacerbated suppression of bacterial growth 24 h after flg22 treatment. However, in the conditions and developmental stage tested in this study, the size and morphology of Iht1-1 seedlings were indistinguishable from wild-type (Figure 5E; Supplemental Figure S9A and B). In addition, Iht1-1 seedlings expressed wild-type levels of the SA-mediated defense marker pathogenesis related-1 (PR1), both after mock and flg22 treatment, suggesting that Iht1-1 seedlings have not yet developed the SA-overaccumulation phenotype observed in adult plants (Supplemental Figure S9C). The low level of intracellular AA in adult *lht1-1* plants

triggers an AA starvation response that induces the ammonium transporter AMT1;1 (Liu et al., 2010). Since AA starvation has been proposed to play an important role in the onset of MTI (Pajerowska-Mukhtar et al., 2012), we tested AMT1:1 expression to assess if AA starvation could explain the exacerbated suppression of bacterial growth in Iht1-1. Our data show that both wild-type and Iht1-1 seedlings expressed similar basal levels of AMT1;1 and induced its expression to the same extent in response to flg22 perception (Supplemental Figure S9D). The strength of the flg22induced defense responses in Iht1-1 was further studied by assessing callose and lignin deposition. Aniline blue and phloroglucinol histochemical staining showed that, in response to flg22 perception, Iht1-1 deposited callose and lignin to a similar extent as wild-type seedlings (Figure 5, D and E; Supplemental Figure \$10). Overall, these data show that no difference in the canonical responses to flg22 perception was observed between Iht1-1 and the wild-type and that the underlying mechanisms that produce the exacerbated suppression of bacterial growth in flg22-elicited Iht1-1 are still unknown.

#### Discussion

### Changes in AA transport are an integral part of the response to MAMP perception

Infected tomato leaves accumulate primary and secondary metabolites thought to be important to define plant resistance or susceptibility to pathogens (Solomon and Oliver, 2001; Solomon and Oliver, 2002; Solomon et al., 2003; Sonawala et al., 2018). The association between susceptibility to virulent pathogens and the increased AA and GABA concentrations reported in these studies suggested a causal link between susceptibility and metabolite accumulation. It is unclear, however, if the change in metabolite concentrations in the whole infected leaf is a signature of an unsuccessful plant defense program or a susceptibility program orchestrated by the pathogen. Several AA found in the tomato leaf apoplast support PstDC3000 growth in vitro (Rico and Preston, 2008), suggesting that their accumulation in infected tomato leaves would favor bacterial growth. However, AA concentrations increased in Arabidopsis leaves inoculated with both virulent and non-virulent PstDC3000 strains, suggesting that both susceptibility and resistance to bacterial infection elicit a similar plant metabolic response (Ward et al., 2010). Recent studies have used chemical or genetic perturbations to elicit defense responses and profile plant metabolites in the absence of infection. The mitogenactivated protein-kinase phosphatase-1 (MKP1) gene encodes a phosphatase that negatively regulates MAMP-triggered signaling (Anderson et al., 2011); the corresponding mkp1 knockout displays enhanced MTI and resistance against PstDC3000. Untargeted mass spectrometry profiling of mkp1 seedling exudates uncovered that among other metabolites, organic acids (citric acid, 4-benzoic acid, and aspartic acid) were present at lower concentrations in mkp1 compared to the wild-type (Anderson et al., 2014). When combined with fructose and applied exogenously, these organic acids showed virulence-inducing activity on *PstDC3000*, and were able to restore bacterial virulence in a dose-dependent manner in *mkp1* and elf26-treated wild-type seedlings. These data suggested that elf26 perception in wild-type plants leads to a decrease in the extracellular concentrations of metabolites that normally allow *PstDC3000* to induce virulence (Anderson et al., 2014). Exudates obtained from *mkp1* and wild-type seedlings contain a complex mix of known and still unidentified metabolites, with several of them represented differentially in *mkp1* (Anderson et al., 2014). This complexity suggests that, in addition to organic acids and sugars, several metabolites whose concentrations change upon MAMP perception could directly or indirectly contribute to suppressing bacterial infections.

Our data show that MAMP perception triggers significant changes in the concentration of extracellular AA, supporting the hypothesis that these changes contribute to plant defense (Supplemental Figure S1; Figure 1 and Table 1). The observed changes in AA concentrations are dynamic, with an inhibition of uptake at early time points (<5 h post-elicitation), followed by an increased AA uptake activity and the concomitant depletion of extracellular AA at later time points (>8 h post-elicitation) (Figures 1 and Importantly, extracellular AA whose concentrations increased soon after flg22-treatment decreased at later time points suggesting that these changes modulate the overall concentration of AA rather than the specific composition (Table 1). While the early inhibition of AA uptake does not seem to operate through gene expression regulation, the late enhanced uptake of AA coincide with the expression of several AA/H \* symporters that were induced in response to flg22 perception (Supplemental Table S1; Figure 2). Among them, LHT1 showed to be essential to execute the enhanced AA uptake during this response (Figure 2; Supplemental Figure S4). Amino acid transport studies in yeast showed that the Arabidopsis LHT1 protein can transport several AA, including Pro, Gln, and Ser, a profile consistent with the changes in AA concentrations detected in our study (Hirner et al., 2006; Rentsch et al., 2007). In addition, LHT1 is expressed in the leaf epidermis and mesophyll cells at the seedling stage, a pattern that is consistent with the increased accumulation of AA in seedling shoots (Figure 1E; Supplemental Figure S2) (Hirner et al., 2006). Similar changes in AA transport were observed in protoplasts obtained from leaf mesophyll cells that directly interact with bacterial pathogens growing in the leaf apoplast. Like in seedlings, the uptake of AA by mesophyll cells was inhibited soon after MAMP perception (Figure 4, B-D), suggesting that mesophyll cells contribute to both, the early decreased AA uptake activity of seedlings (Figure 4A) and the increased concentration of extracellular AA in seedlings exudate 4 h after flg22 treatment (Figure 1A and Table 1). Overall, our data suggest that changes in extra- and intracellular concentration of AA are integral responses to MAMP perception. The concentrations of individual extracellular AA are

determined by the relative activity of both AA exporters and importers. While exporters are likely facilitators that move AA passively downward a concentration gradient (Ladwig et al., 2012; Müller et al., 2015; Besnard et al., 2016; Besnard et al., 2018), AA/H<sup>+</sup> symporters recapture extracellular AA (Frommer et al., 1995; Yang et al., 2020). Thus, the decreased AA uptake that follows the first 1-3 h upon MAMP perception likely suffice to transiently increase the extracellular concentrations of AA (Figures 1, B, C, D and 4). Indeed, when the plasma membrane H<sup>+</sup> gradient was dissipated by CCCP treatment, a rapid increase in the concentrations of extracellular AA was observed (Figure 2, A and B). The transient inhibition of AA uptake in response to flg22 perception could result from cytosolic Ca<sup>2+</sup> influx and anions efflux, together or independently of the flg22mediated inhibition of the plasma membrane H<sup>+</sup>-ATPase (Jeworutzki et al., 2010; Elmore and Coaker, 2011). The consequent increase in the extracellular pH could inhibit the activity of the AA/H symporters thereby producing the accumulation of AA outside the cells (Felix et al., 1999; Gómez-Gómez et al., 1999; leworutzki et al., 2010). Once the ion fluxes return to basal levels, the restored electrochemical gradient would then allow AA/H+ symporters to work and lower the extracellular concentrations of AA.

It is unclear, however, if these changes take place in mature plants and if and how they operate under natural infection conditions. The dynamic nature of the changes in transport activity and extracellular concentrations of AA suggests that timing is important. Since infected leaves start to accumulate AA 12 h after inoculation with virulent or avirulent bacteria (Ward et al., 2010), it seems plausible that reverting the MAMP-elicited changes could contribute to the success of pathogenic bacteria. Indeed, if virulent bacteria manage to suppress the early MAMP-elicited inhibition and the later increase in AA uptake activity, they could induce a slow but sustained increase in the concentrations of extracellular AA that could favor host colonization. Such a scenario is consistent with the sustained increased of total AA concentration in Arabidopsis leaves between 12 h and 18 h after inoculation with virulent bacteria compared to the overall drop in concentrations observed between 12 h and 18 h after inoculation with avirulent bacteria (Ward et al., 2010).

### Salicyclic acid signaling positively regulate the expression of AA/H \* symporters

The role of SA signaling in plant defense is best understood in the context of ETI, where cytosolic plant receptors detect microbial effectors and trigger a rapid SA burst essential to execute PCD. Although ETI does not entirely rely on PCD (Clough et al., 2000; Coll et al., 2010; Coll et al., 2011), it often provides infected plants with the last resource to stop localized infections. Unlike ETI, however, the MAMP-elicited SA burst typically does not lead to PCD, and the role of SA seems to be limited to the reinforcement of an flg22-elicited signaling sector that is susceptible to T3E-mediated

suppression (Tsuda et al., 2008; Tsuda et al., 2009). Our data uncovered an important role for SA-mediated signaling in regulating the expression AA/H+ symporters and AA uptake. SA signaling contributes to inducing the expression of AA/H<sup>+</sup> symporters that play a role in lowering extracellular concentrations of AA (Figures 2, C, F and 3, C-E). Further confirming the role of SA signaling in AA transport regulation, we uncovered that mutants with altered SA levels, and hence, SA-mediated signaling capacity, differ in their AA uptake activity in both non-elicited and elicited conditions (Figures 3 and 4; Supplemental Figure S5). In addition, our data show that SA signaling contributes to basal and induced expression of LHT1 and other AA/H+ symporters, each one perhaps contributing a modest but significant uptake activity that becomes evident when comparing AA uptake in wild-type versus sid2-2 or npr1 seedlings or mesophyll cell protoplasts (Figures 3 and 4). The compromised AA uptake 24 h after MAMP perception could partially explain the enhanced susceptibility to bacterial infections of sid2-2 and other mutants with defective SA signaling. Transport defects could alter AA concentrations inside and outside the cells, and consequently the speed and the magnitude of the MAMP-elicited changes in AA transport activity, which could allow bacterial pathogens to suppress plant defense responses early in the infection and take advantage of the extracellular AA at later time points to support robust bacterial growth. The opposite SA-mediated signaling phenotype of cpr1 and sid2-2 positively correspond with both their resistance to P. syringae infections and their AA uptake activity. Yet, further studies will be necessary to determine if the AA transport phenotype of cpr1 and sid2-2 translates into differences in the speed and magnitude of changes in the extracellular concentration of AA and how that impacts bacterial growth in these mutants.

## Increased concentrations of extracellular AA contribute to suppressing bacterial growth during

Several pieces of evidence obtained in this study suggested a positive association between bacterial growth and AA availability. Amino acid concentration in seedling exudates or lysates of seedlings corresponded with bacterial growth (Figure 5, A and B). Exogenous supplementation of individual AA whose extracellular concentrations dropped 24 h after flg22 treatment rescued bacterial growth in exudates of flg22-treated wild-type seedlings (Supplemental Table S2). This association was also evident when comparing bacterial growth in wild-type and Iht1-1 mock-treated seedlings (Figure 5C; Supplemental Figure S8). These observations suggested that the long-term increase in AA uptake that removes extracellular AA would suppress bacterial growth by perhaps depriving the pathogen of needed nutrients. However, in contradiction with this hypothesis, when MTI was elicited 24 h prior to bacterial inoculation of seedlings, Iht1-1 was more effective at suppressing bacterial growth than the wild-type (Figure 5C; Supplemental Figure S8).

This observation could be explained by an exacerbated flg22-induced defense responses in Iht1-1. However, canonical responses to MTI elicitation, namely callose and lignin deposition, and SA-mediated PR-1 expression, were induced similarly in Iht1-1 and in wild-type seedlings (Figure 5, D and E; Supplemental Figure S9C). In addition, unlike in adult plants, no morphological evidence of SA-mediated enhanced resistance phenotypes (e.g. stunted growth) was observed in Iht1-1 at the seedling stage (Supplemental Figure S9, A and B). These data suggest that exacerbated flg22-induced responses do not account for the exacerbated suppression of bacterial growth in Iht1-1. Nevertheless, we cannot rule out that MAMP-elicited responses that we have not tested in this study could contribute to the exacerbated suppression of PsmES4326 observed in Iht1-1, and further studies will be needed to test this possibility.

The exacerbated suppression of bacterial growth observed in flg22-treated *lht1-1* indicates that low concentrations of extracellular AA are not essential to suppress bacterial growth, at least when MTI is elicited 24 h prior to bacterial inoculation. On the contrary, the evidence suggests that high concentrations of extracellular AA help suppress the growth of invading bacteria.

Based on the evidence collected in this study, it seems likely that the MTI-elicited suppression of bacterial growth relies on a defensive response that involves increasing the concentrations of extracellular AA alongside an offensive response that involves the onset of other MAMP-elicited responses such as the synthesis of toxic metabolites. The defensive responses could impact bacterial metabolism preventing the onset of survival programs needed to counter offensive plant responses. In support of this hypothesis, previous studies have revealed both, that AA availability regulates (p) ppGpp synthesis and survival responses (Traxler et al., 2008), and that (p) ppGpp responses control survival and virulence programs in P. syringae (Chatnaparat et al., 2015a; Chatnaparat et al., 2015b). Although the biological function of the enhanced uptake of AA and the low extracellular AA content observed 24 h upon MAMP perception remains unknown, we hypothesize it could allow plant cells to restore AA homeostasis in anticipation of future encounters with microbes. If such readiness pertains the fast increase in concentration of extracellular AA, the compromised reuptake of AA would allow Iht1-1 to build high AA concentrations in the leaf apoplast constitutively, bypassing the need for fast AA release. Further studies will be needed to test this hypothesis.

#### Materials and methods

#### Plant material

Arabidopsis thaliana ecotype Col-0 and T-DNA insertional lines (Col-0 background) were obtained from Arabidopsis Biological Resource Center, Ohio State University. Whenever available, two independent alleles of previously uncharacterized insertional lines were tested. The SALK lines used in this study were obtained and indexed by Alonso et al. (2003).

Wild-type Col-0 (CS1092); fls2-1 (SALK 026801) (Jaillais et al., 2011); efr-1 (SALK 044334c) (Zipfel et al., 2006); aap3-1 (SALK 148822) (Marella et al., 2013); aap4 (Wiscseq DsLox351C05.0); Iht1-1 (SALK\_034566) (Hirner et al., 2006); cat1 (SALK 087921) (Yang et al., 2014); Iht7-1 (SALK 027033); lht7-2 (SALK 043012); lht10 (SALK 114616); (SALK 067508). The sid2-2 mutant was a gift from Mary Wildermuth at the University of California, Berkeley; npr1-1 and cpr1-1 mutant were a gift from Xinnian Dong at Duke University. Polymerase chain reaction genotyping and gene expression primers are listed in Supplemental Table S3. Agarose gel images of PCR genotyping and RT-PCR gene expression tests are shown in Supplemental Figure S11.

### Plant growth and MAMP treatments

Seedlings were grown in 12-well tissue culture plates as previously published with few modifications (Danna et al., 2011). Seeds were sterilized in 10% v/v bleach (2 min, twice) and washed three times with sterile water. After 48 h incubation at  $4^{\circ}$ C in the dark for stratification purposes, 15–20 seeds were dispensed into wells of 12-well tissue culture plates (BD Falcon; 353043) containing 1 mL of liquid MS medium. Seedlings were grown for 10 days (replacing medium at Day 8) at 23°C, 80% humidity (to prevent medium evaporation) in plant growth incubators (Conviron Adaptis A1000) under 100  $\mu$ E·m<sup>-2</sup>·s<sup>-1</sup> energy and a 16 h photoperiod. Ten-day-old seedlings were mock-treated with water or treated with MAMPs by pipetting a water solution of synthetic peptides (GenScript) into the wells (1- $\mu$ M final concentration of flg22 or elf26).

### Uptake of proline, glutamine, serine, and glucose in seedlings

Arabidopsis seeds were surface sterilized in 10% bleach and kept in dark at 4°C for 2 days before sowing on MS phytoagar plates. The plates were incubated vertically in growth chambers for 3 days. Seedlings were then transferred to 12well culture plates with fresh MS liquid medium (pH 5.7) and incubated as described above (Plant growth and MAMP treatment). Seeds of cpr1 were germinated in MS liquid medium side by side with the corresponding wild-type controls. Every well of a 12-well plate contained 10 seedlings, and the uptake was normalized by dry weight. Liquid MS medium was changed on day eight after sowing. On Day 10, 1-μM flg22 or elf26 peptide (final concentration) was added to the seedlings. The same volume of sterile water was added to the mock group. When indicated, 100-µM CCCP (final concentration) was added to the seedling 40 min before uptake starts. The uptake protocol was modified from Pratelli et al. (2010). Seedlings were washed in MS liquid medium and then incubated in fresh MS medium with 100 µM cold Proline, cold glutamine, or cold serine, and 3.7 kBq of the corresponding U-3H-radiolabeled AA (Perkin Elmer). Plates with seedlings were then transferred to a growth chamber and incubated under slow shaking at 23°C, 80% relative humidity, and 30 μE.m<sup>-2</sup>.s<sup>-1</sup> for 15 min. The uptake was stopped by washing seedlings with 0.2 mM CaSO<sub>4</sub> twice.

To assess uptake in roots and shoots separately, seedlings were washed and sectioned right below the hypocotyl, and counts per minute (CPMs) were measured separately. Samples were then lyophilized, ground into powder using glass beads and a Tissue Lyser (QIAGEN) and digested in 1 mL of 10% bleach overnight. Chlorine was removed by drying the samples at 55°C overnight before resuspending the samples in 200 µL of scintillation cocktail (Ultima Gold; Perkin Elmer) and transferring them to a 96-well Isoplate-96 microplate (PerkinElmer). Radioactivity (counts per minute) was measured with a MicroBeta Trilux Scintillation Counter (Perkin Elmer). Glucose uptake was assessed as described above using <sup>14C</sup>Glc (Perkin Elmer) and 100-μM cold glucose. Unless otherwise indicated in the figure legends, seedlings were treated with water (mock) or MAMPs for 8 h and allowed to uptake <sup>3H</sup>Pro for 3 h. For <sup>3H</sup>Gln, <sup>3H</sup>Ser, and <sup>14C</sup>Glc uptake activity, seedlings were treated for 24 h with water (mock) or MAMPs and allowed to uptake <sup>3H</sup>Gln, <sup>3H</sup>Ser, and <sup>14C</sup>Glc for 0.5 h before processing the samples to count CPMs.

### Quantification of free AA in seedling exudate

Murashige and Skoog medium containing seedling exudates was collected by pipetting the liquid medium out of the wells containing 15–20 11-day-old seedlings grown as described above (see Plant growth and MAMP treatments). Total AA concentration in exudates was quantified with the commercial kit "L-Amino Acid Quantitation Colorimetric/Fluorometric" (BioVision).

### AA profiling

Samples were collected as indicated above Quantification of free AA in seedling exudate) and analyzed at the University of Virginia-Biomolecular Analysis Facility Core following a standard protocol (Nemkov et al., 2019). Serial dilutions of standards of every AA were ran for every analysis. Five µL of samples were injected into a ultra-highperformance liquid-chromatography (UHPLC) (Ultimate 3000, Thermo, San Jose, CA, USA) and separated through a 3 min isocratic elution (5% acetonitrile, 95% water, 0.1% formic acid) on a 1.7 µm C18 column (Kinetex XB-C18, Phenomenex, Torrance, CA, USA) at 250 µL min<sup>-1</sup> and 25°C. High-resolution mass spectrometry analysis was performed using a triple quadrupole orbitrap mass spectrometer (Q-Exactive HF-X, Thermo Scientific).

### Leaf mesophyll protoplast preparations and uptake of radiolabeled AA

Arabidopsis protoplasts were obtained from 4-week-old Arabidopsis plants grown under 12 h light photoperiod,  $100~\mu\text{E.m}^{-2}.\text{s}^{-1}$  light energy,  $24^{\circ}\text{C}$ , and 70% humidity, following a standard protocol (Yoo et al., 2007). For uptake assays, protoplasts incubated in mannitol 400 mM + MgCl<sub>2</sub> 15 mM + 2-(N-morpholino)-ethanesulfonic acid (MES) 4 mM solution overnight were transferred to 12-well culture plates with 1 mL of mannitol 500 mM + MES 4 mM + KCl 20 mM buffer per well. For MTI elicitation, 1  $\mu$ M (final) flg22

or sterile water (mock) was added to protoplasts suspension. Plates with protoplasts were then kept in growth chambers under dim light (20  $\mu E.m^{-2}.s^{-1}$ ) and gently rocking for 3 h before adding 100  $\mu M$  (final) cold AA, and 3.7 kBq (final) U- $^3H$ - of the corresponding radiolabeled AA. Samples were taken at different time points as indicated in figure legends and lysed in reporter lysis buffer (Promega E397A). For normalization purposes, aliquots of the lysates were used for protein quantification with Bradford assays. The samples were then bleached and CPMs were quantified as described previously for seedlings. CPMs were normalized by mg of protein.

### RNA work and gene expression analysis

Seedlings were grown as described above (see Plant growth and MAMP treatments) flashed frozen in liquid nitrogen followed by Trizol-RNA extraction protocol (Invitrogen) with metal beads and a bead beater (Tissue Lyser, QIAGEN). RNA samples were treated with DNAse-I (Promega) for genomic DNA decontamination. For nanoString analysis, three RNA samples (one sample per experiment from three independent experiments) were used; hybridizations of samples with fluorescent probe sets were performed following standard protocols in a nCounter Hybridization and reading Station as previously (Geiss et al., 2008). Raw fluorescent counts were analyzed and normalized by the expression of Actin2 and log-transformed using nSolver software (nanoString Technologies Inc). LHT10 probes were not included in the original nanoString probe set, hence, LHT10 expression was quantified via RT-qPCR.

For RT–qPCR, cDNA template was synthesized with M-MLV (Promega) retro-transcriptase and random oligohexamers (Invitrogen). Actin2 expression was used for normalization. For protoplasts, RNA was extracted with RNeasy Plant Mini Kit (QIAGEN). pcr primers used for genotyping and RT–qPCR primers used for gene expression analysis are listed in Supplemental Table S3. nanoString probes for gene expression analysis are listed in Supplemental Table S4. The expression of every gene in response to flg22 was assessed as relative to ACT2 (At3g18780). When gene expression was assessed across multiple genotypes, the relative expression of each gene was normalized by the relative expression of the same gene in mock or nontreated wild-type seedlings.

#### MTI elicitation and seedling infection assay

Ten-day-old seedlings were grown as indicated above (plant growth and MAMP treatments), mock-treated with water or treated with 1-μM flg22 for 24 h, and then inoculated with the auto luminescent *P. syringae* pv. maculicola strain ES4326 optical density 600nm (OD<sub>600nm</sub> = 0.0002) carrying the *luxABCDE* operon (Fan et al., 2007). The infection proceeded in the exact same conditions the seedlings were grown prior to the inoculation. Thirty hours later, infected seedlings were removed from each well, quickly dried on paper towels to remove surface liquid, and transferred to sterile 2 mL round-bottom tubes. Samples (15–20 seedlings from each well) were weighted, and 400 μL of sterile water plus three spherical 5 mm stainless steel beads were added

to each tube. Seedlings were ground with a beat beater (Tissue Lyser, QIAGEN) at 25 shakes/s for 3 min. To determine bacterial counts, aliquots of 100  $\mu$ L of seedling lysates were transferred to 96-well microtiter plates (CELLSTAR, Greiner Bio) and luminescence was assessed as CPMs in a Wallack 1450 Microbeta TriLux (PerkinElmer). Bacterial titer was estimated by converting CPMs into colony forming unit (CFUs) using a CPMs/CFUs experimentally determined conversion standard (Supplemental Figure S12). The infection conditions (inoculum and the time point) were set up to assess luminescence (CPMs) when both CFUs and CPMs increase constantly ( $R^2$  is close to 1) during the infection.

### Bacterial growth in liquid exudates of seedlings or seedling lysates

PsmES4326 (OD<sub>600nm</sub> = 0.002) harboring the luxABCDE operon (Fan et al., 2007) was streaked out of fresh Luria brothagar plates and cultured in King's B liquid medium for about 4 h at 28°C until it reached an OD600 nm of 0.5-0.7. Bacteria were pelleted and washed three times with sterile water and resuspended to the desired OD<sub>600 nm</sub> in sterile MS medium. Liquid seedling exudates or seedling lysates were aliquoted in white solid-bottom 96-well sterile plates (CELLSTAR Greiner Bio) and were inoculated with OD<sub>600 nm</sub> = 0.0002 (inoculation titter) and the growth was constantly monitored as luminescence (RLUs) with a multimode microplate reader (Molecular Devices, SpectraMax i3x) at 28°C with constant orbital shaking. Luminescence was recorded every 30 min for a 12 h period, and bacterial doubling time was calculated from > 10 time points (5 h of growth) where bacterial luminescence increased at a constant rate (Supplemental Figure S12). The TREND function in the Excel software (Microsoft Office) was used to obtain the B value needed to calculate doubling time in each condition. The B value is the slope "y" value of the X, Y scattered plot equation. Doubling time was calculated as the natural logarithm of 2 (0.693) divided by B.

#### Callose and lignin deposition staining

Seeds were sown in MS liquid medium and grown for six days. MTI was elicited with 1 µM (final) flg22 or elf26 by adding the purified peptides to the medium. Seedlings were grown for another two days to allow for callose and lignin depositions to become evident. Seedlings were then fixed with acetic acid: ethanol (1:3) for at least 1 h. For callose staining, seedlings were washed in 150 mM K<sub>2</sub>HPO<sub>4</sub> for 30 min. Aniline blue (Sigma-Aldrich) 0.01% (final concentration) was added to 150 mM K<sub>2</sub>HPO<sub>4</sub> to obtain the staining solution. Seedlings were submerged in the staining solution for 3 h in the dark. Images were taken with an EVOS Cell Imaging System (Thermo Fisher) using DAPI filter and 4× or 10× lenses. For lignin staining, seedlings were stored in 100% ethanol after fixing. Before imaging, samples were rehydrated in 70% ethanol, 50% ethanol, 30% ethanol for 30 min each step before transferring to water. The staining solution was prepared by adding phloroglucinol to a 15% HCl acid solution. Seedlings were positioned on glass slides without a cover and covered with staining solution. Soon after adding staining solution, dark field images of seedlings were taken with  $1 \times$  and  $0.25 \times$  FWD 60 mm lenses in a Zeiss AXIO Zoom.V16 microscope (Zeiss).

### Data analyses

The statistical analysis of the data was performed with GraphPad Prism and R. All data were subjected to Fligner-Killeen test in R to assess homoscedasticity. When Fligner-Killeen P-values were above 0.05, indicative of equal variances across compared groups, statistical significance between two groups was calculated using two-tailed t test (i.e. t test) or one-way analysis of variance (ANOVA) for multiple groups. When Fligner-Killeen P-values were below 0.05, indicative of unequal variances, statistical significance was calculated using Welch t test for two groups. When multiple t test was used to compare more than two groups of data, the two-stage step-up method (Benjamini et al., 2006) was used for false discovery rate analysis with a 1% cutoff (Q = 0.01). Welch and Brown-Forsythe ANOVA test was used for the analysis of multiple group comparisons with different variances. Asterisks indicate statistically significant differences at P-values of \*P < 0.05, \*\*P < 0.01, and \*\*\*P < 0.001. Unless otherwise indicated in the figure legend, similar results were obtained in three independent experiments.

#### **Accession Numbers**

Sequence data from this article can be found in the GenBank/EMBL data libraries under the accession numbers provided in Supplemental Table S3.

#### Supplemental data

The following materials are available in the online version of this article.

**Supplemental Figure S1.** The perception of flg22 and elf26 elicits similar changes in AA uptake.

**Supplemental Figure S2.** <sup>3H</sup>Pro uptake in roots and shoots of wild-type seedlings.

**Supplemental Figure S3.** Total extracellular AA in exudates of seedlings 24 h after flg22 treatment.

**Supplemental Figure S4.** LHT1 contributes to both flg22-and elf26-induced enhanced AA uptake.

**Supplemental Figure S5.** Salicylic acid-mediated signaling contributes to sustaining Gln uptake in mock-treated seedlings.

**Supplemental Figure S6.** Perception of flg22 in wild-type seedlings induces the expression of AA/H<sup>+</sup> symporters.

**Supplemental Figure S7.** Perception of flg22 in wild-type leaf mesophyll protoplasts.

**Supplemental Figure S8.** MAMP-elicited suppression of bacterial growth.

**Supplemental Figure S9.** Ten-day-old *lht1* seedling morphology and gene expression.

**Supplemental Figure S10.** Aniline staining of callose in wild-type and lht1 mock- (M) or flg22- (F) treated seedlings.

**Supplemental Figure S11.** Genotyping and gene expression analysis of T-DNA insertional lines

**Supplemental Figure S12.** Luminescence versus CFU standard

**Supplemental Table S1.** The perception of flg22 induces the expression of AA/H+ symporters

**Supplemental Table S2.** *Psm*ES4326 doubling time (h) in exudates of flg22-treated seedlings supplemented with 10 mM individual AA.

**Supplemental Table S3.** Genes, mutants, and primers used in this study.

Supplemental Table S4. nanoString probe set.

### **Acknowledgments**

We thank A. Saghatelian, G. Jander, M. Haribal, F. M. Ausubel, X-C Zhang, Y. Millet, S. Djonovic, M. Jain, N. Madhusudhan, M. Fischbach and B. Sattely for technical support and helpful discussions on early exploratory stages of this study; D. Parichy for his assistance on lignin deposition imaging.

### **Funding**

This work was supported by the University of Virginia 4-VA grant SG00409 (to C. H. Danna) and by the National Science Foundation CAREER Award IOS-1943120 grant (to C. H. Danna). F. R. Rossi thanks the National Scientific and Technical Research Council (CONICET—Argentina) and International Union for Biochemistry and Molecular Biology (IUBMB) Wood—Whelan Fellowship for travel financial support.

Conflict of interest statement. The authors declare no conflict of interest.

#### References

- Adams-Phillips L, Briggs AG, Bent AF (2009) Disruption of poly(ADP-ribosyl)ation mechanisms alters responses of Arabidopsis to biotic stress. Plant Physiol 152: 267–280
- Alonso JM, Stepanova AN, Leisse TJ, Kim CJ, Chen H, Shinn P, Stevenson DK, Zimmerman J, Barajas P, Cheuk R, et al. (2003)
  Genome-wide insertional mutagenesis of Arabidopsis thaliana. Science 301: 653-657
- Anderson JC, Bartels S, Besteiro MAG, Shahollari B, Ulm R, Peck SC (2011) Arabidopsis MAP kinase phosphatase 1 (AtMKP1) negatively regulates MPK6-mediated PAMP responses and resistance against bacteria. Plant J 67: 258–268
- Anderson JC, Wan Y, Kim Y-M, Pasa-Tolic L, Metz TO, Peck SC (2014) Decreased abundance of type III secretion system-inducing signals in Arabidopsis mkp1 enhances resistance against Pseudomonas syringae. Proc Natl Acad Sci USA 111: 6846–6851
- Asai T, Tena G, Plotnikova J, Willmann MR, Chiu WL, Gomez-Gomez L, Boller T, Ausubel FM, Sheen J (2002) Map kinase signalling cascade in Arabidopsis innate immunity. Nature 415: 977–983
- Bender CL, Stone HE, Sims JJ, Cooksey DA (1987) Reduced pathogen fitness of Pseudomonas syringae pv. tomato Tn5 mutants defective in coronatine production. Physiol Mol Plant Pathol 30: 273–283
- **Benjamini Y, Krieger AM, Yekutieli D** (2006) Adaptive linear step-up procedures that control the false discovery rate. Biometrika **93**: 491–507

- Besnard J, Pratelli R, Zhao C, Sonawala U, Collakova E, Pilot G, Okumoto S (2016) UMAMIT14 is an amino acid exporter involved in phloem unloading in Arabidopsis roots. J Exp Bot 67: 6385–6397
- Besnard J, Sonawala U, Maharjan B, Collakova E, Finlayson SA, Pilot G, McDowell J, Okumoto S (2021) Increased expression of UMAMIT amino acid transporters results in activation of salicylic acid dependent stress response. Front Plant Sci 11: 606386
- Besnard J, Zhao C, Avice J-C, Vitha S, Hyodo A, Pilot G, Okumoto S (2018) Arabidopsis UMAMIT24 and 25 are amino acid exporters involved in seed loading. J Exp Bot 69: 5221–5232
- **Bourbouloux A, Raymond P, Delrot S** (1998) Effects of salicylic acid on sugar and amino acid uptake. J Exp Bot **49**: 239–427
- Bowling SA, Guo A, Cao H, Gordon AS, Klessig DF, Dong X (1994)
  A mutation in Arabidopsis That leads to constitutive expression of systemic acquired resistance. Plant Cell 6: 1845
- **Brooks DM, Bender CL, Kunkel BN** (2005) The pseudomonas syringae phytotoxin coronatine promotes virulence by overcoming salicylic acid-dependent defences in Arabidopsis thaliana. Mol Plant Pathol **6**: 629–639
- **Bush DR, Langston-Unkefer PJ** (1988) Amino acid transport into membrane vesicles isolated from zucchini: Evidence of a proton-amino Acid symport in the plasmalemma. Plant Physiol **88**: 487–90
- Cao H, Glazebrook J, Clarke JD, Volko S, Dong X (1997) The Arabidopsis NPR1 gene that controls systemic acquired resistance encodes a novel protein containing ankyrin repeats. Cell 88: 57–63
- Chatnaparat T, Li Z, Korban SS, Zhao Y (2015a) The bacterial alarmone (p)ppGpp is required for virulence and controls cell size and survival of P seudomonas syringae on plants. Environ Microbiol 17: 4253–4270
- Chatnaparat T, Li Z, Korban SS, Zhao Y (2015b) The stringent response mediated by (p)ppGpp is required for virulence of pseudomonas syringae pv. tomato and its survival on tomato. Mol Plant-Microbe Interact 28: 776–789
- Chezem WR, Memon A, Li F-S, Weng J-K, Clay NK (2017) SG2-Type R2R3-MYB transcription factor MYB15 controls defense-induced lignification and basal immunity in Arabidopsis. Plant Cell 29: 1907–1926
- Clay NK, Adio AM, Denoux C, Jander G, Ausubel FM (2009) Glucosinolate metabolites required for an arabidopsis innate immune response. Science **323**: 95–101
- Clough SJ, Fengler KA, Yu IC, Lippok B, Smith RK, Bent AF (2000)
  The Arabidopsis dnd1 "defense, no death" gene encodes a mutated cyclic nucleotide-gated ion channel. Proc Natl Acad Sci U S A 97: 9323–8
- Coll NS, Epple P, Dangl JL (2011) Programmed cell death in the plant immune system. Cell Death Differ 18: 1247–56
- Coll NS, Vercammen D, Smidler A, Clover C, Van Breusegem F, Dangl JL, Epple P (2010) Arabidopsis type I metacaspases control cell death. Science 330: 1393–1397
- Danna CH, Millet YA, Koller T, Han S-W, Bent AF, Ronald PC, Ausubel FM (2011) The Arabidopsis flagellin receptor FLS2 mediates the perception of Xanthomonas Ax21 secreted peptides. Proc Natl Acad Sci USA 108: 9286–9291
- Delaney T, Uknes S, Vernooij B, Friedrich L, Weymann K, Negrotto D, Gaffney T, Gut-Rella M, Kessmann H, Ward E, et al. (1994) A central role of salicylic acid in plant disease resistance. Science 266: 1247–1250
- Denoux C, Galletti R, Mammarella N, Gopalan S, Werck D, De Lorenzo G, Ferrari S, Ausubel FM, Dewdney J (2008) Activation of defense response pathways by OGs and Flg22 elicitors in Arabidopsis seedlings. Mol Plant 1: 423–445
- **Elmore JM, Coaker G** (2011) The role of the plasma membrane H+-ATPase in plant-microbe interactions. Mol Plant **4**: 416–427
- Fan J, Crooks C, Lamb C (2007) High-throughput quantitative luminescence assay of the growth in planta of Pseudomonas syringae

- chromosomally tagged with Photorhabdus luminescens luxCDABE. Plant J **53**: 393–399
- Felix G, Duran JD, Volko S, Boller T (1999) Plants have a sensitive perception system for the most conserved domain of bacterial flagellin. Plant J 18: 265–276
- Frommer WB, Hummel S, Unseld M, Ninnemann O (1995) Seed and vascular expression of a high-affinity transporter for cationic amino acids in Arabidopsis. Proc Natl Acad Sci U S A 92: 12036–12040
- Gazzarrini S, Lejay L, Gojon A, Ninnemann O, Frommer WB, von Wirén N (1999) Three functional transporters for constitutive, diurnally regulated, and starvation-induced uptake of ammonium into Arabidopsis roots. Plant Cell 11: 937–947
- Geiss GK, Bumgarner RE, Birditt B, Dahl T, Dowidar N, Dunaway DL, Fell HP, Ferree S, George RD, Grogan T, et al. (2008) Direct multiplexed measurement of gene expression with color-coded probe pairs. Nat Biotechnol 26: 317–325
- Gómez-Gómez L, Felix G, Boller T (1999) A single locus determines sensitivity to bacterial flagellin in Arabidopsis thaliana. Plant J 18: 277–284
- Greenberg JT, Guo A, Klessig DF, Ausubel FM (1994) Programmed cell death in plants: a pathogen-triggered response activated coordinately with multiple defense functions. Cell 77: 551–563
- Hauck P, Thilmony R, He SY (2003) A pseudomonas syringae type III effector suppresses cell wall-based extracellular defense in susceptible Arabidopsis plants. Proc Natl Acad Sci U S A 100: 8577–8582
- Hirner A, Ladwig F, Stransky H, Okumoto S, Keinath M, Harms A, Frommer WB, Koch W (2006) Arabidopsis LHT1 is a high-affinity transporter for cellular amino acid uptake in both root epidermis and leaf mesophyll. Plant Cell 18: 1931–1946
- Jaillais Y, Belkhadir Y, Balsemão-Pires E, Dangl JL, Chory J (2011) Extracellular leucine-rich repeats as a platform for receptor/coreceptor complex formation. Proc Natl Acad Sci U S A 108: 8503–8507
- Jeworutzki E, Roelfsema MRG, Anschütz U, Krol E, Elzenga JTM, Felix G, Boller T, Hedrich R, Becker D (2010) Early signaling through the Arabidopsis pattern recognition receptors FLS2 and EFR involves Ca2 + -associated opening of plasma membrane anion channels. Plant J 62: 367–378
- Jirage D, Tootle TL, Reuber TL, Frosts LN, Feys BJ, Parker JE, Ausubel FM, Glazebrook J (1999) Arabidopsis thaliana PAD4 encodes a lipase-like gene that is important for salicylic acid signaling. Proc Natl Acad Sci U S A **96**: 13583–13588
- Ladwig F, Stahl M, Ludewig U, Hirner AA, Hammes UZ, Stadler R, Harter K, Koch W (2012) Siliques are red1 from Arabidopsis acts as a bidirectional amino acid transporter That is crucial for the amino acid homeostasis of siliques. Plant Physiol 158: 1643–1655
- Lecourieux D, Lamotte O, Bourque S, Wendehenne D, Mazars C, Ranjeva R, Pugin A (2005) Proteinaceous and oligosaccharidic elicitors induce different calcium signatures in the nucleus of tobacco cells. Cell Calcium 38: 527–538
- Liu G, Ji Y, Bhuiyan NH, Pilot G, Selvaraj G, Zou J, Wei Y (2010) Amino acid homeostasis modulates salicylic acid-associated redox status and defense responses in Arabidopsis. Plant Cell 22: 3845–3863
- **Lu Y, Tsuda K** (2021) Intimate association of PRR- and NLR-mediated signaling in plant immunity. Mol Plant Microbe Interact **34**: 3–14
- Lynne Reuber T, Plotnikova JM, Dewdney J, Rogers EE, Wood B, Ausubel FM (1998) Correlation of defense gene induction defects with powdery mildew susceptibility in Arabidopsis enhanced disease susceptibility mutants. Plant J 16: 473–485
- Marella HH, Nielsen E, Schachtman DP, Taylor CG (2013) The amino acid permeases AAP3 and AAP6 are involved in root-knot nematode parasitism of Arabidopsis. Mol Plant-Microbe Interact 26: 44–54

- Millet YA, Danna CH, Clay NK, Songnuan W, Simon MD, Werck-Reichhart D, Ausubel FM (2010) Innate immune responses activated in Arabidopsis roots by microbe-associated molecular patterns. Plant Cell 22: 973–990
- Müller B, Fastner A, Karmann J, Mansch V, Hoffmann T, Schwab W, Suter-Grotemeyer M, Rentsch D, Truernit E, Ladwig F, et al. (2015) Amino acid export in developing Arabidopsis seeds depends on UmamiT facilitators. Curr Biol 25: 3126–3131
- Nemkov T, D'Alessandro A, Hansen KC (2019) Three-minute method for amino acid analysis by UHPLC and high-resolution quadrupole orbitrap mass spectrometry. Amino Acids 47: 2345–2357
- Nicaise V, Roux M, Zipfel C (2009) Recent advances in PAMP-triggered immunity against bacteria: Pattern recognition receptors watch over and raise the alarm. Plant Physiol **150**: 1638–1647
- Nobori T, Velásquez AC, Wu J, Kvitko BH, Kremer JM, Wang Y, He SY, Tsuda K (2018) Transcriptome landscape of a bacterial pathogen under plant immunity. Proc Natl Acad Sci U S A 115: E3055–E3064
- O'Leary BM, Neale HC, Geilfus C-M, Jackson RW, Arnold DL, Preston GM (2016) Early changes in apoplast composition associated with defence and disease in interactions between Phaseolus vulgaris and the halo blight pathogen Pseudomonas syringae Pv. phaseolicola. Plant Cell Environ 39: 2172–2184
- Okumoto S, Pilot G (2011) Amino acid export in plants: A missing link in nitrogen cycling. Mol Plant 4: 453–463
- Okumoto S, Schmidt R, Tegeder M, Fischer WN, Rentsch D, Frommer WB, Koch W (2002) High affinity amino acid transporters specifically expressed in xylem parenchyma and developing seeds of Arabidopsis. J Biol Chem 277: 45338–45346
- Pajerowska-Mukhtar KM, Wang W, Tada Y, Oka N, Tucker CL, Fonseca JP, Dong X (2012) The HSF-like transcription factor TBF1 is a major molecular switch for plant growth-to-defense transition. Curr Biol 22: 103–112
- Park DH, Mirabella R, Bronstein PA, Preston GM, Haring MA, Lim CK, Collmer A, Schuurink RC (2010) Mutations in γ-amino-butyric acid (GABA) transaminase genes in plants or Pseudomonas syringae reduce bacterial virulence. Plant J 64: 318–330
- Pratelli R, Voll LM, Horst RJ, Frommer WB, Pilot G (2010)
  Stimulation of nonselective amino acid export by glutamine dumper proteins. Plant Physiol 152: 762–773
- Rahme LG, Mindrinos MN, Panopoulos NJ (1992) Plant and environmental sensory signals control the expression of hrp genes in Pseudomonas syringae pv. phaseolicola. J Bacteriol 174: 3499–3507
- Rentsch D, Hirner B, Schmelzer E, Frommer WB (1996) Salt stress-induced proline transporters and salt stress-repressed broad specificity amino acid permeases identified by suppression of a yeast amino acid permease-targeting mutant. Plant Cell 8: 1437–1446
- Rentsch D, Schmidt S, Tegeder M (2007) Transporters for uptake and allocation of organic nitrogen compounds in plants. FEBS Lett 581: 2281–2289
- **Rico A, Preston GM** (2008) Pseudomonas syringae pv. tomato DC3000 uses constitutive and apoplast-induced nutrient assimilation pathways to catabolize nutrients that are abundant in the tomato apoplast. Mol Plant-Microbe Interact **21**: 269–282
- **Solomon PS, Oliver RP** (2001) The nitrogen content of the tomato leaf apoplast increases during infection by Cladosporium fulvum. Planta **213**: 241–249
- **Solomon PS, Oliver RP** (2002) Evidence that γ-aminobutyric acid is a major nitrogen source during Cladosporium fulvum infection of tomato. Planta **214**: 414–420
- **Solomon PS, Tan K-C, Oliver RP** (2003) The nutrient supply of pathogenic fungi; a fertile field for study. Mol Plant Pathol **4**: 203–210
- Sonawala U, Dinkeloo K, Danna CH, McDowell JM, Pilot G (2018) Review: Functional linkages between amino acid transporters and plant responses to pathogens. Plant Sci 277: 79–88
- Su Y-H, Frommer WB, Ludewig U (2004) Molecular and functional characterization of a family of amino acid transporters from Arabidopsis. Plant Physiol 136: 3104–3113

- Traxler MF, Summers SM, Nguyen H-T, Zacharia VM, Hightower GA, Smith JT, Conway T (2008) The global, ppGpp-mediated stringent response to amino acid starvation in Escherichia coli. Mol Microbiol 68: 1128–48
- Tsuda K, Sato M, Glazebrook J, Cohen JD, Katagiri F (2008) Interplay between MAMP-triggered and SA-mediated defense responses. Plant J 53: 763–775
- Tsuda K, Sato M, Stoddard T, Glazebrook J, Katagiri F (2009) Network properties of robust immunity in plants. PLoS Genet 5: e1000772
- Volko SM, Boller T, Ausubel FM (1998) Isolation of new Arabidopsis mutants with enhanced disease susceptibility to pseudomonas syringae by direct screening. Genetics 149: 537–548
- Ward JL, Forcat S, Beckmann M, Bennett M, Miller SJ, Baker JM, Hawkins ND, Vermeer CP, Lu C, Lin W, et al. (2010) The metabolic transition during disease following infection of Arabidopsis thaliana by Pseudomonas syringae pv. tomato. Plant J 63: 443–457
- Wildermuth MC, Dewdney J, Wu G, Ausubel FM (2001) Isochorismate synthase is required to synthesize salicylic acid for plant defence. Nature 414: 562–565
- Xin X-F, He SY (2013) Pseudomonas syringae pv. tomato DC3000: A model pathogen for probing disease susceptibility and hormone signaling in plants. Annu Rev Phytopathol 51: 473–498
- Yamada K, Saijo Y, Nakagami H, Takano Y (2016) Regulation of sugar transporter activity for antibacterial defense in Arabidopsis. Science 354: 1427–1430

- Yang G, Wei Q, Huang H, Xia J (2020) Amino acid transporters in plant cells: A brief review. Plants 9: 967
- Yang H, Postel S, Kemmerling B, Ludewig U (2014) Altered growth and improved resistance of Arabidopsis against Pseudomonas syringae by overexpression of the basic amino acid transporter AtCAT1. Plant, Cell Environ 37: 1404–1414
- Yao X, Nie J, Bai R, Sui X (2020) Amino acid transporters in plants: Identification and function. Plants 9: 972
- Yoo S-D, Cho Y-H, Sheen J (2007) Arabidopsis mesophyll protoplasts: a versatile cell system for transient gene expression analysis. Nat Protoc 2: 1565–1572
- Yu X, Lund SP, Scott RA, Greenwald JW, Records AH, Nettleton D, Lindow SE, Gross DC, Beattie GA (2013) Transcriptional responses of Pseudomonas syringae to growth in epiphytic versus apoplastic leaf sites. Proc Natl Acad Sci U S A 110: E425–E434
- Zhang W, He SY, Assmann SM (2008) The plant innate immunity response in stomatal guard cells invokes G-protein-dependent ion channel regulation. Plant J 56: 984–996
- Zipfel C, Kunze G, Chinchilla D, Caniard A, Jones JDG, Boller T, Felix G (2006) Perception of the bacterial PAMP EF-Tu by the receptor EFR restricts agrobacterium-mediated transformation. Cell 125: 749–760
- Zipfel C, Robatzek S, Navarro L, Oakeley EJ, Jones JDG, Felix G, Boller T (2004) Bacterial disease resistance in Arabidopsis through flagellin perception. Nature 428: 764–7